An Investigation of the Storage and Biosynthesis of Phenylpropenes in Sweet Basil[1]

David R. Gang*, Jihong Wang, Natalia Dudareva, Kyoung Hee Nam, James E. Simon, Efraim Lewinsohn, and Eran Pichersky

Department of Biology, University of Michigan, Ann Arbor, Michigan 48109–1048 (D.R.G., J.W., K.H.N., E. P.); Horticulture Department, Purdue University, West Lafayette, Indiana 47907 (N.D.); Department of Plant Science, Rutgers University, New Brunswick, New Jersey 08901 (J.E.S.); and Aromatic, Medicinal, and Spice Crops Unit, Newe Ya'ar Research Center, Agricultural Research Organization, P.O. Box 1021, Ramat Yishay 30095, Israel (E.L.)

Plants that contain high concentrations of the defense compounds of the phenylpropene class (eugenol, chavicol, and their derivatives) have been recognized since antiquity as important spices for human consumption (e.g. cloves) and have high economic value. Our understanding of the biosynthetic pathway that produces these compounds in the plant, however, has remained incomplete. Several lines of basil (*Ocimum basilicum*) produce volatile oils that contain essentially only one or two specific phenylpropene compounds. Like other members of the Lamiaceae, basil leaves possess on their surface two types of glandular trichomes, termed peltate and capitate glands. We demonstrate here that the volatile oil constituents eugenol and methylchavicol accumulate, respectively, in the peltate glands of basil lines SW (which produces essentially only eugenol) and EMX-1 (which produces essentially only methylchavicol). Assays for putative enzymes in the biosynthetic pathway leading to these phenylpropenes localized many of the corresponding enzyme activities almost exclusively to the peltate glands in leaves actively producing volatile oil. An analysis of an expressed sequence tag database from leaf peltate glands revealed that known genes for the phenylpropanoid pathway are expressed at very high levels in these structures, accounting for 13% of the total expressed sequence tags. An additional 14% of cDNAs encoded enzymes for the biosynthesis of *S*-adenosyl-methionine, an important substrate in the synthesis of many phenylpropenes. Thus, the peltate glands of basil appear to be highly specialized structures for the synthesis and storage of phenylpropenes, and serve as an excellent model system to study phenylpropene biosynthesis.

Two classes of compounds, terpenoids and phenylpropenes (allylphenols/propenylphenols), make up the bulk of plant volatile oils (also referred to as "essential oils") and contribute to, or define outright, the particular properties of many spices and herbs. For example, the terpenoid menthol, the major constituent of peppermint, gives this herb its cool, peppery aroma and flavor. The major constituent of cloves (one of the spices that led Columbus to sail from Spain, [Guenther, 1949]), on the other hand, is the phenylpropene eugenol (see Fig. 1), which gives this spice its pungent, distinctive aroma. Eugenol makes up 70% to 90% of the essential oil and 15% of the dry weight of clove buds (Myrtaceae; Guenther, 1949). Eugenol is also found in significant amounts in cinnamon and cinnamon leaves (Gildemeister and Hoffmann, 1913) and in lesser amounts in nutmeg (Gildemeister and Hoffmann, 1913) and pepper

corns, which together make up the four oldest known spices (Gildemeister and Hoffmann, 1913).

The adaptive value of the toxic (i.e. defensive) properties of the phenylpropenes are likely responsible for the widespread distribution of these chemicals among the angiosperms, and humans have made extensive use of these properties to further protect their plants and food stocks. Eugenol serves as a good example. It is an antibacterial compound that inhibits the growth of many significant food-borne pathogenic bacteria (Miyao, 1975; Blank et al., 1987; Moleyar and Narasimham, 1992; Bara and Vanetti, 1995). Eugenol is an effective antifungal agent, acting as a fungistatic (Ryu and Holt, 1993) or fungicidal (Karapinar and Aktug, 1987; Adams and Weidenborner, 1996) compound, depending on the fungus. Nematodes are susceptible to eugenol, being killed at low dosages (Chatterjee et al., 1982; Sangwan et al., 1990). Plants treated with such low concentrations exhibited no ill effects (Bala and Sukul, 1987; Matsuoka et al., 1993). The pungent eugenol also has a marked insect antiherbivory effect (Sisk et al., 1996; Obeng-Ofori and Reichmuth, 1997). On the other hand, the pleasant, fresh-smelling methyleugenol is an important component of many floral scents, attracting pollinating moths and beetles in particular,

* Corresponding author; e-mail dgang@umich.edu; fax 734–647–0884.
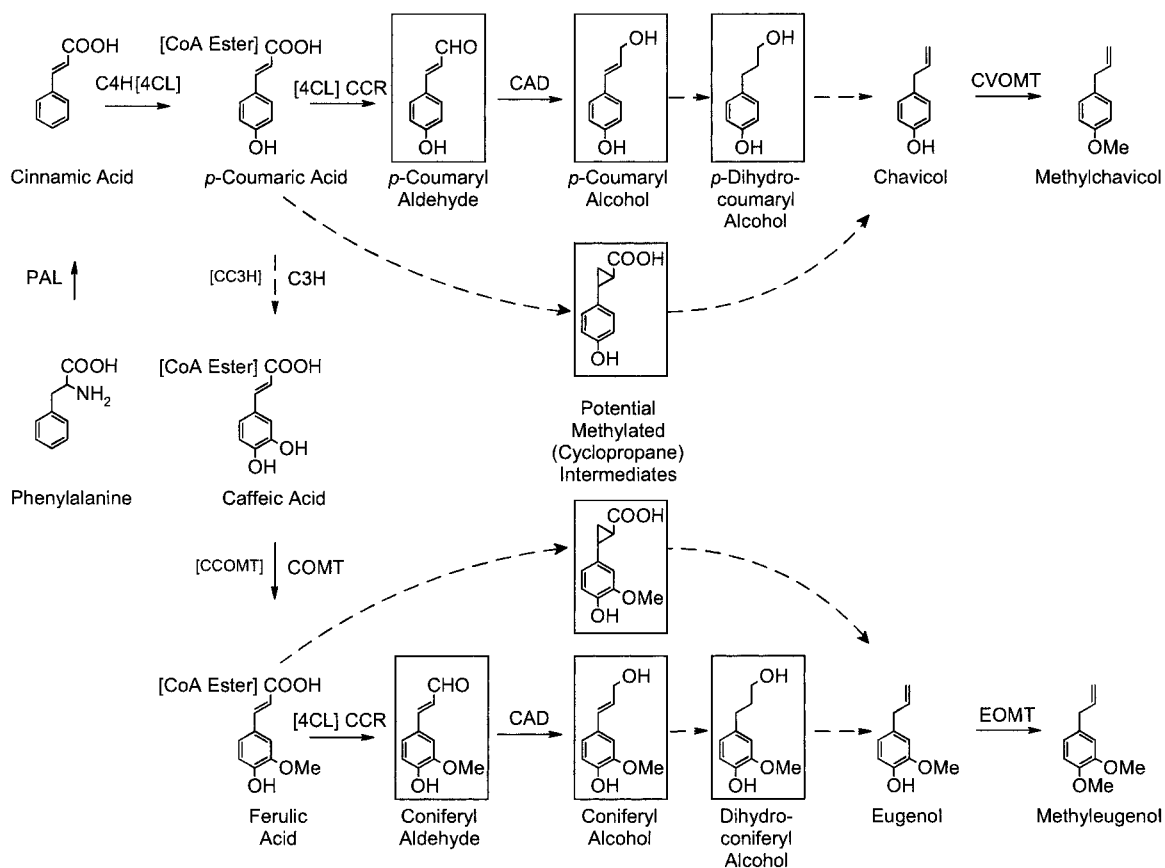
Figure 1. Proposed biosynthetic pathway to phenylpropenes in basil. Enzymes are as follows: C4H, cinnamate 4-hydroxylase; C3H, *p*-coumarate 3-hydroxylase; CC3H, *p*-coumaroyl-CoA 3-hydroxylase; CCR, cinnamoyl-CoA reductase; and CAD, cinnamyl alcohol dehydrogenase. Dotted lines indicate hypothetical reactions; hypothetical intermediates are boxed. The phenylpropanoid pathway involving methylations of the CoA esters (as opposed to the free acids) is shown in brackets.

as well as being a female pheromone mimic for several fruit flies (Shukla and Prasad, 1985).

A large body of literature exists describing the biosynthesis of terpenoid constituents of herb essential oils, with many of the proteins and genes involved in this latter pathway having been purified and cloned (Chappell, 1995; Bohlmann et al., 1998; Wise et al., 1998). However, surprisingly little is known about the biosynthesis of eugenol and chavicol, the simplest phenylpropenes, and their derivatives. Labeling experiments of leaf segments with radioactive Phe indicated that Phe is their initial precursor (Manitto et al., 1974; Klischies et al., 1975; Manitto et al., 1975; Senanayake et al., 1977). Based on these results, two proposed biosynthetic pathways to these and related phenylpropenes are illustrated in Figure 1. The first committed step to the phenylpropenes, the de-amination of Phe to give cinnamic acid, is likely to be catalyzed by the well-known and widely distributed enzyme Phe ammonia lyase (PAL), just as is the case for the biosynthesis of other phenylpropanoids. The next steps are likely to be the formation of *p*-coumaric and ferulic acids from cinnamic acid (addition of 4-hydroxyl and 3-methoxyl functionalities). These reactions may involve the prior formation of the coenzyme A (CoA) esters, or they may proceed directly, with the substrates in the free acid form; both pathways have been proposed to be involved in the formation of the monolignols required for lignification (Boudet et al., 1998). The next steps in the production of eugenol and chavicol after the formation of ferulic and coumaric acids, respectively, are not known. Conflicting reports based only on feeding radioactive precursors to whole leaf tissues suggested that eugenol is formed from the monolignol precursor coniferyl alcohol (Klischies et al., 1975; see Fig. 1) or is instead formed via an undefined mechanism involving methylation and decarboxylation (Manitto et al., 1974, 1975; Senanayake et al., 1977) of the hydroxycinnamic acids (see potential methylated intermediates in Fig. 1). Confirmation of the last step in the formation of methylchavicol and methyleugenol, the addition of the methyl group to the 4-OH, has been reported recently (Wang et al., 1997; Wang and Pickersky, 1999; Lewinsohn et al., 2001). Thus, the critical intermediary steps in chavicol and eugenol biosynthesis are still an open question.

Although cloves have historically been the largest source for eugenol, they are not readily amenable to biochemical inquiry: cloves are the dried flower buds produced by the tropical tree *Eugenia caryophyllata*, which takes many years to mature. *Ocimum* species, by contrast, are small annual or perennial plants that are readily cultivated in the greenhouse or in the field and have been shown to produce high levels of phenylpropenes in their essential oils, up to 90% of the total (the essential oil of basil [*Ocimum basilicum*] also often contains monoterpenes such as linalool and camphor; Pareek et al., 1980; Charles et al., 1990; Grayer et al., 1996). Breeding lines of sweet basil that produce essentially only eugenol (line SW), only methylchavicol (line EMX-1), methylchavicol and methyleugenol in approximately equal amount (line R1), or almost no phenylpropenes at all, but instead almost exclusively methylcinnamate (line MC) as the phenylpropanoid-derived components of their essential oils have been obtained.

Many plants (e.g. geranium, tobacco, and cotton) possess specialized glands known as glandular trichomes on the surface of their leaves, and the presence of such glands is often correlated with exudation of defense compounds and pest resistance (Navasero and Ramaswamy, 1991; Walters et al., 1991). In the Lamiaceae, which includes basil and mint, two classes of secretory glandular trichomes can be found. Peltate glands, which are made of a stalk cell attached to the leaf, four to eight secretory cells attached to the stalk cell, and an oil sac ("subcuticular space") above the secretory cells, are believed to contain the stored essential oil components (Gershenzon et al., 1992; Werker et al., 1993; McCaskill and Croteau, 1995; Bohlmann et al., 1998). Capitate glandular trichomes, on the other hand, consist of one or two cells that sit atop a stalk of one to several cells. These glands possess only a small oil sac, if one is present at all. Peltate glands have been examined in several species and have been shown to produce monoterpene and sesquiterpene compounds (Gershenzon et al., 1992; McCaskill and Croteau, 1995; Bohlmann et al., 1998). However, glandular synthesis and/or accumulation of phenylpropenes have not yet been directly demonstrated in the Lamiaceae or in any other taxa. In this paper we show that the peltate glands are the site of storage, and most likely biosynthesis, of the phenylpropenes found in basil leaves. Basil peltate glands thus constitute an excellent system to study the biosynthesis of phenylpropenes.

RESULTS

Basil Peltate Glandular Trichomes Contain Phenylpropenes

The basic structure of basil leaf glands had been reported before (Werker et al., 1993). There are two types of glands, peltate and capitate. Each peltate gland consists of four secretory cells that form a disc and are covered with a loose-fitting, overlying oil sac membrane (Fig. 2A, no. 1). As the gland develops, the secretory disc cells expand, followed by the oil sac membrane, which at first appears wrinkled and creased along the fissures between the apices of the secretory cells (Fig. 2B). The oil sac then becomes completely inflated as it fills with the essential oil constituents (Fig. 2C). At this stage of gland development the secretory cells are no longer visible, although crease marks are still observable in the wrinkly sac, reflecting the quadrilateral symmetry of the secretory disc. Then as the whole leaf and its epidermal cells continue to expand, the peltate glands become recessed into the surface of the leaf (Fig. 2, D, E, and G). A similar developmental pattern occurs for the basil capitate glands, except that these glands contain only one or two secretory cells, the oil sac does not grow to be nearly as large, and though partially recessed, they do not sink nearly as far into the surface of the leaf. On basil sepals, as well as on the leaves of many other members of the Lamiaceae (such as *Mentha* × *piperita* and *Nepeta racemosa*), the peltate glands are not recessed at all (Fig. 2F; Gershenzon et al., 1992).

Although a previous report correlated gland density with essential oil content (Werker et al., 1993), further evidence that the glands were indeed the site of phenylpropene storage and synthesis was not obtained. To investigate the location of phenylpropene storage in basil lines EMX-1 and SW, whole and ground leaves of different sizes, and leaves from which the glands had been removed by abrasion (see "Materials and Methods"), were extracted with methyl *tert*-butyl ether (MTBE) and the resulting extracts were analyzed by gas chromatography/mass spectrometry (GC/MS) for essential oil composition (see Fig. 3). Essential oil profiles obtained from ground and whole leaves were very similar to each other. For the EMX-1 line, the major essential oil component is methylchavicol (Fig. 3A, peak 2), which makes up greater than 50% of the MTBE-extractable essential oil in this line. The absolute values vary depending on the age of the leaves, on the age of plant (for leaves of the same size), and on the growth conditions (e.g. growth chamber versus greenhouse grown). It is interesting that we found that methyleugenol was also produced by this line (Fig. 3A, peak 4), but at very minor amounts (<1%). The major MTBE-extractable essential oil compounds from expanding SW leaves were eugenol (51.5%), linalool (11.4%), and α-bergamotene (11.7%; Fig. 3C).

Abrasive treatment to remove the glands from the abaxial and adaxial leaf surfaces of both lines caused a significant reduction in the amounts of essential oil constituents measured (Fig. 4A). This effect was more pronounced in the SW line, where a 6-fold reduction in eugenol content was observed after such treatment, than in the EMX-1 line, where only about a
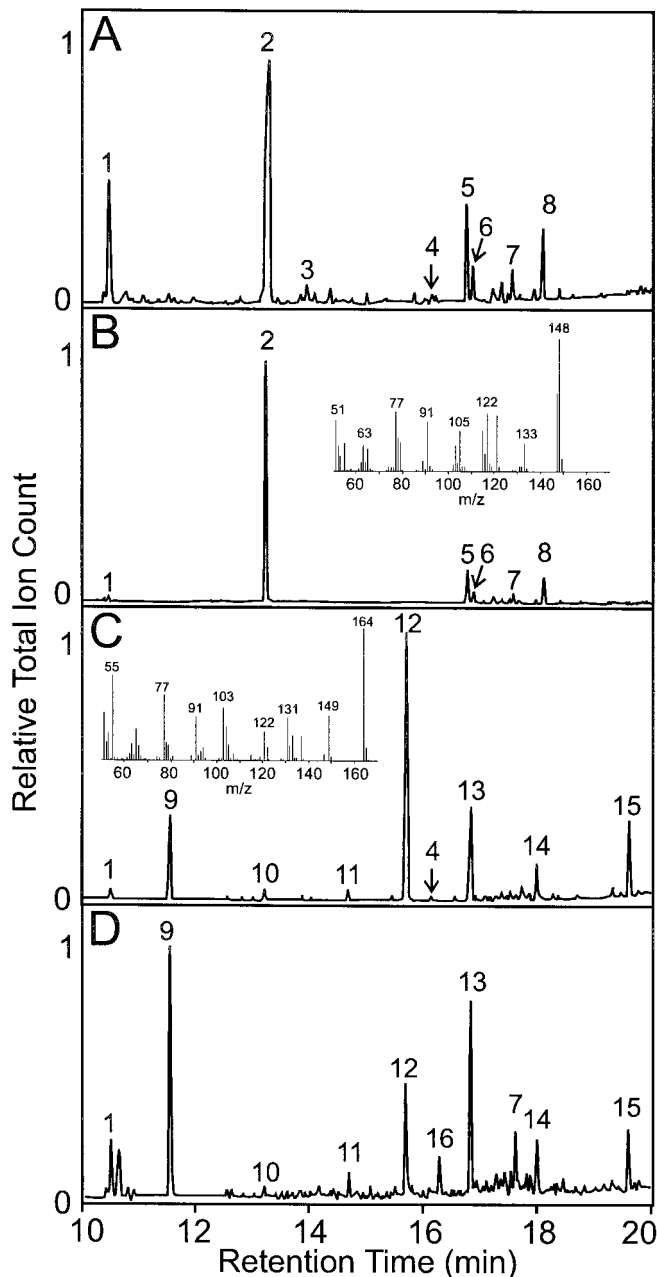
Figure 2. Morphology of basil peltate and capitate glands. A, SEM of adaxial surface of a very young EMX-1 leaf (<0.5 cm long) showing the high density at initiation of peltate and capitate glands on basil leaves. 1, Peltate gland early in development; 2, gland primordium. B, Closer view of peltate and capitate glands from same leaf as in A. The 4- and 2-fold symmetries, respectively, of each gland type are clearly visible, as are two perpendicular creases and the wrinkled folds of the immature oil sac membrane. C, Side view of a fully expanded peltate gland on a young EMX-1 leaf (1.5 cm long). D, Peltate gland on the surface of a young EMX-1 leaf, showing the fine structure of the oil sac, including the two perpendicular remnant creases left by the four underlying secretory cells. E, Adaxial surface of an expanding EMX-1 leaf (2 cm long). The peltate gland, whose oil sac is partially deflated, is recessed into the surface of the leaf. Stomatal guard cells are visible (arrow). F, Structure of glands on the surface of developing sepals from line SW, revealing the stalk cell connecting each gland to the leaf. Several non-glandular trichomes can be seen in the background. Again, the oil sac on the peltate gland is partially deflated. G, Light micrograph of an EMX-1 leaf cross-section (adaxial surface up) stained with toluidine blue showing how deeply the peltate glands (arrow) are recessed into the leaf.
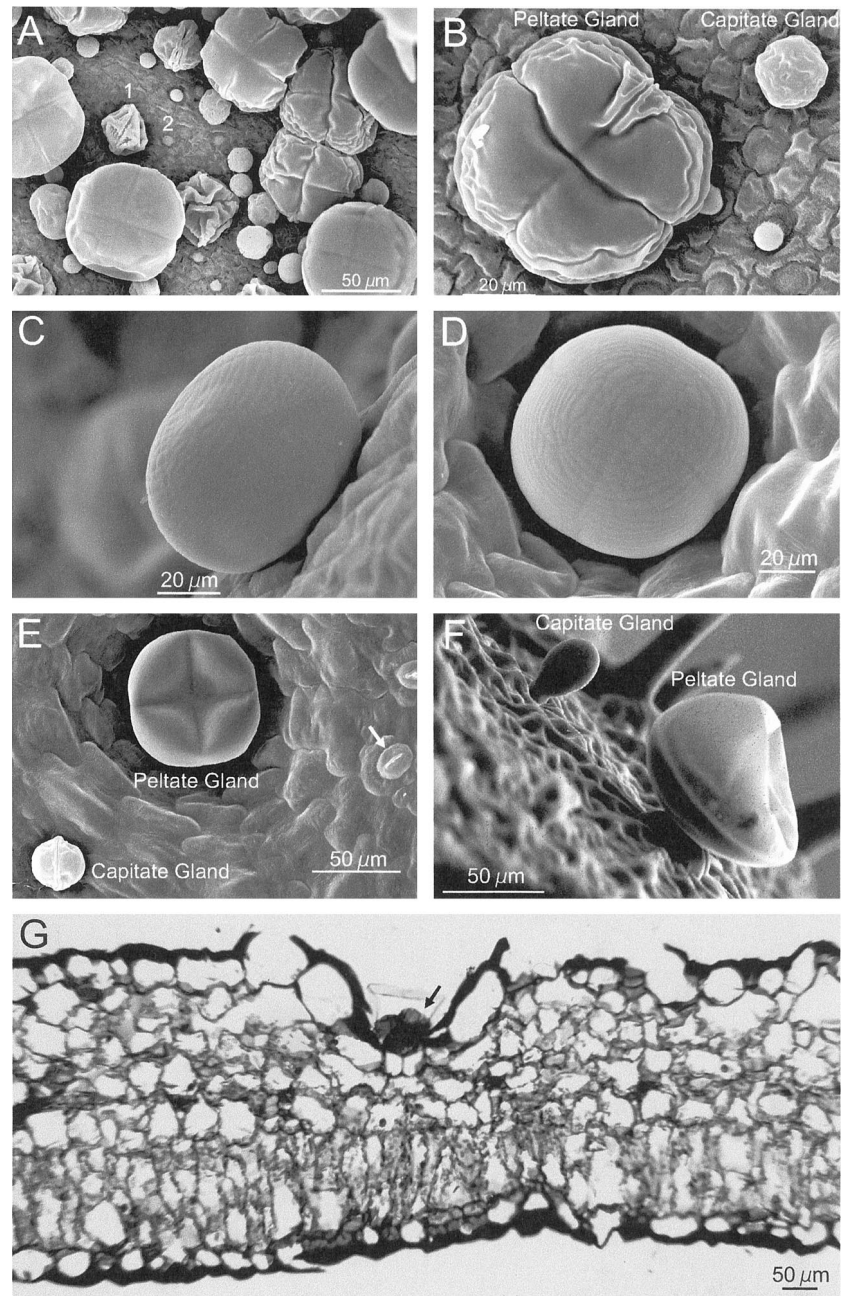
2-fold reduction in methylchavicol content was observed. A similar level of reduction was also noted for linalool, the major terpenoid constituent of basil essential oil (data not shown). Analysis of variance (ANOVA) determined that the differences observed in the mean values for eugenol and methylchavicol content in whole leaves versus in leaves after abrasive treatment are significant, with P values of 3.4×10^{-5} and 0.029 for the SW and EMX-1 lines, respectively. Careful microscopic evaluation of leaves treated for gland removal explained the difference in reduction between the two basil lines. Abrasion with cotton swabs of the abaxial and adaxial surfaces of leaves from the SW line removed most (>75%) of the glands from both leaf surfaces without any further damage to the epidermis (abrasion with fine brushes or latex gloves was not as effective as abrasion with cotton swabs at removing glands from either line). Identical treatment of the EMX-1 line, however, removed almost all of the glands from only the first side abraded, whether it be the adaxial or abaxial (again, without any additional damage to the epidermal cell layer). Very few of the glands appeared to be removed from the side abraded second because they appeared to be greatly recessed into the leaves after abrasion of the first leaf surface and therefore were protected from abrasion. Because about one-half of the glands were removed from the treated EMX-1

line support the same conclusion for the site of eugenol storage.

To further verify that glands on the surface of the leaves store phenylpropenes, we used stretched glass pipettes to extract a small droplet of essential oil from sacs of individual peltate glands (observed on the leaf surface under a dissecting microscope) and then analyzed the oil by GC/MS. Although the yields of extracted oil were extremely small, the major essential oil components (methylchavicol for line EMX-1 and eugenol and linalool for line SW) were clearly identified in these extracts (data not shown). Individual capitate glands yielded too little oil for detection

We next optimized a procedure (Gershenzon et al., 1992) for removing the peltate and capitate glands from the leaf surface without damaging them, and for separating them from all other leaf material (except for some non-glandular hairy trichomes, which contain no cytoplasm). In this procedure, first applied to mint leaves (Gershenzon et al., 1992; McCaskill and Croteau, 1995) and then adapted by us for basil, the leaf surface is abraded with small glass beads to yield intact capitate or peltate glands (minus the stalk cell)—clusters of intact, live secretory cells, separate from the rest of the leaf. Initial separation yields a mixture of the peltate and capitate glands (Fig. 5), and the two gland types can be further separated from each other to yield each gland type free from
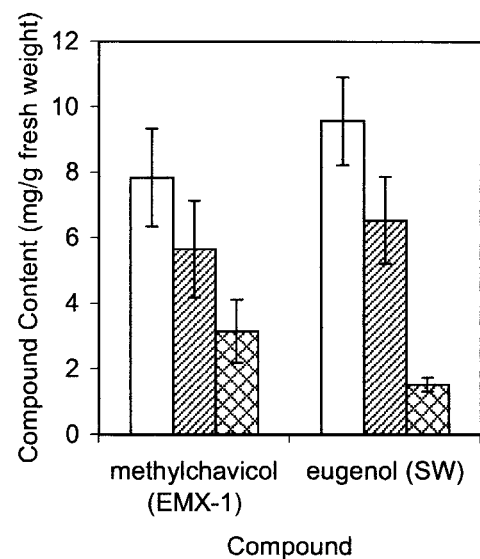

Figure 3. GC analysis of essential oil constituents from developing leaves from basil lines EMX-1 (A) and SW (C) and from peltate glands (B and D) isolated from these two lines, respectively. Mass spectra inserted into B and C are for the major peaks, 2 and 12, respectively. Major essential oil components that were identified by in-line mass spectrometry are labeled by number: 1, cineole; 2, methylchavicol; 3, chavicol; 4, methyleugenol; 5, β-caryophyllene; 6, β-farnesene; 7, germacrene isomer I; 8, humulene; 9, linalool; 10, α-terpineol; 11, fenchyl acetate; 12, eugenol; 13, α-bergamotene; 14, germacrene isomer II; 15, δ-cadinol; and 16, β-elemene.

leaves and this caused a 2-fold reduction in methylchavicol content, methylchavicol is apparently stored almost exclusively (if not entirely) in the glands, and not in the epidermal cell layer. The results for the SW

Figure 4. Effect of abrasive treatment to remove glands on content of the major phenylpropene in the essential oil of young basil leaves (1–2 cm in length) from lines EMX-1 (for methylchavicol) and SW (for eugenol). White bar, Non-treated leaves; diagonal-line filled bar, leaves rinsed with 100% (w/v) ethanol; cross-hatch filled bar, leaves from which the glands had been removed by manual abrasion and then rinsed with 100% (w/v) ethanol. Extracts from ground individual leaves, after the appropriate indicated treatment, were analyzed by GC/MS for essential oil content. Values, in milligrams of phenylpropene per gram of fresh leaf weight, are averages from leaves from five plants. Error bars are SE of the mean.
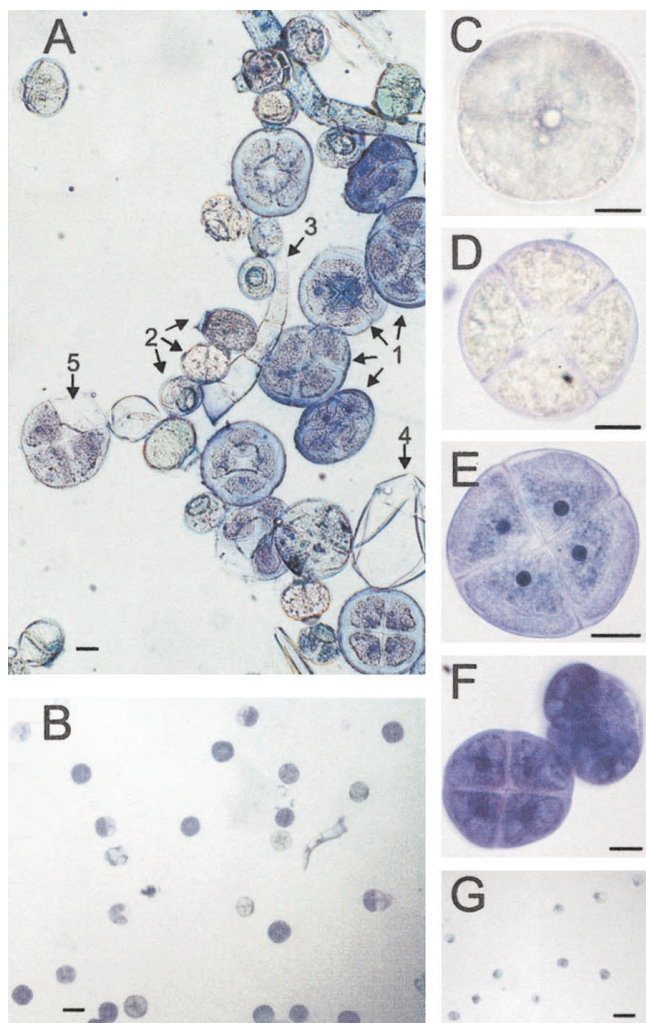
Figure 5. Light micrographs of basil glands isolated from line EMX-1. A, Mixture of glandular trichomes prior to final purification step, showing the difference in morphology between the peltate (1) and capitate gland (2) types in basil. Some non-glandular hairs are also visible (3), as are oil sac ghosts (4) and a few broken glands (5). Scale = 20 μm. B, Purity of the peltate glands after final purification, scale = 80 μm. C and D, Isolated peltate glands, not stained with toluidine blue, with focus set at the interface between the gland disc cells and the overlying oil sac (C) and through the middle of the disc of secretory cells (D), scale = 20 μm. E and F, Isolated peltate glands stained with toluidine blue, showing the prominent nucleoli (E) and a comparison of the cross-sectional and transverse views of the disc of secretory cells (F), scale = 20 μm. G, Purity of the capitate glands after final purification, scale = 80 μm.

contaminating tissues (Fig. 5, B and G). Gland isolation preparations from the EMX-1, SW, and other lines yielded essentially identical looking gland mixtures. The peltate glands, as observed in the light microscope, are discs of four cells (see Fig. 5, A, arrows labeled 1, and B), whereas the isolated capitate glands consist of one or two cells connected to a stalk cell (Fig. 5, A, arrows labeled 2, and G). Hairy trichomes are also present (arrow 3) in the initial

gland preparations, as are oil sac "ghosts" (Fig. 5A, arrow 4), which are broken off of the peltate gland discs during the bead abrasion procedure. These oil sac remnants are not always removed from the peltate glands, but often remain partially or even completely attached through the entire gland isolation procedure. Some of the glands are damaged by the procedure (Fig. 5A, arrow 5), but these make up a small proportion (<5%) of the isolated glands (data not shown). The isolated peltate secretory cells are highly cytoplasmic and contain only small vacuoles (Fig. 5, C and D). When stained with toluidine blue (Fig. 5, E and F), the nucleoli are very prominent, indicating that the secretory cells possess high metabolic activity.

Analysis of the material extracted from capitate glands indicated that they contain only very small amounts of straight-chain hydrocarbons and small-chain alcohols (data not shown). The peltate glands, on the other hand, contain large stores of the respective phenylpropenes found in each basil line (Fig. 3, B and D). To be specific, the isolated glands of the EMX-1 line contain almost the identical composition as the whole leaf, with the only major difference observed for cineole (compare Fig. 3A to 3B). In the isolated peltate glands of the SW line, the same essential oil components were present as the ones found in whole leaf, although the relative amounts of eugenol changed from 51.5% in whole leaf to 13.3% in the glands (Fig. 3, C and D). These changes in relative proportions of certain compounds in the isolated glands may reflect a difference between its concentration in the sac and its concentration in the disc cells themselves, because many (but not all) of the isolated glands lack an intact sac. Alternatively, these changes may be due to the greater solubility of these compounds in the aqueous buffer system used during the gland isolation procedure. Most important, however, is the great similarity in qualitative oil composition found in MTBE extracts of isolated glands and whole expanding leaves.

Peltate Glandular Trichomes Contain Enzymes of the Phenylpropene Biosynthetic Pathway

Crude protein extracts obtained from young leaves, from isolated peltate glands, and from isolated capitate glands (all of which were obtained from the same batch of leaves) were assayed for activity for the first and last enzymes in the pathway leading to the phenylpropenes, as well as for some additional enzymes of the phenylpropanoid pathway that might also be involved in phenylpropene biosynthesis. These enzymes included PAL, eugenol *O*-methyl transferase (EOMT), chavicol *O*-methyltransferase (CVOMT), 4-coumarate:CoA ligase (4CL), caffeic acid *O*-methyltransferase (COMT), and caffeoyl-CoA *O*-methyltransferase (CCOMT; see Fig. 1 for the reactions catalyzed by these enzymes). Extracts from

Table I. *Specific activities[a] of phenylpropanoid pathway enzymes assayed in tissues from basil cultivars EMX-1 and SW*

Source	PAL	4CL	COMT	CCOMT	EOMT	CVOMT
EMX-1 Peltate glands	0.223 ± 0.009	46.27 ± 0.94	11.17 ± 0.03	42.40 ± 0.76	67.43 ± 1.63	72.29 ± 2.86
EMX-1 Whole leaf	0.026 ± 0.004	18.48 ± 2.13	0.48 ± 0.02	0.85 ± 0.20	1.90 ± 0.24	1.85 ± 0.23
EMX-1 Stripped leaf	0.023 ± 0.003	8.94 ± 1.72	0.41 ± 0.03	0.50 ± 0.08	0.68 ± 0.06	0.85 ± 0.06
SW Peltate glands	0.420 ± 0.012	120.30 ± 1.32	7.04 ± 0.31	31.51 ± 0.96	0.51 ± 0.16	0.51 ± 0.21
SW Whole leaf	Not detected	12.77 ± 3.01	0.25 ± 0.02	0.78 ± 0.07	Not detected	Not detected
SW Stripped leaf	Not detected	9.21 ± 1.80	0.27 ± 0.03	0.48 ± 0.03	Not detected	Not detected

[a] Note: all values in picomoles product formed per second (pkat) mg^{-1}, ±SEM.

whole young leaves of EMX-1 and SW lines possessed activity for all of these enzymes (Table I), with the exception that PAL, EOMT, and CVOMT activities were not detectable in extracts from SW whole leaves. The lack of EOMT and CVOMT activities is not surprising because the SW line accumulates eugenol, does not synthesize methylchavicol, and produces only very small amounts of methyleugenol (see Fig. 3, C and D).

Capitate glands isolated from EMX-1 and SW leaves were tested for PAL, COMT, EOMT, and CVOMT activities. None of these enzyme activities were detectable in protein extracts from this gland type. However, extracts from the capitate glands did have comparable specific activity with extracts from peltate glands and whole leaf tissue for malate dehydrogenase, a so-called housekeeping enzyme (specific activity values were 21.3, 15.6, and 15.3 picomoles product formed per second (pkat) mg^{-1} for extracts from capitate glands, peltate glands, and whole leaf, respectively). Thus, the capitate glands on basil leaves do appear to be metabolically active.

In contrast with the capitate glands, the specific activities for all of the assayed phenylpropanoid pathway enzymes in crude extracts from basil peltate glands were significantly higher (at the 95% confidence level) than in extracts from basil whole leaf tissue (see Table I). This was true for the EMX-1 and SW lines. The ratios of specific activity for the enzymes found in crude extracts from peltate glands versus from whole leaves (Fig. 6A) range from 3- to 10-fold higher activity in the peltate glands for PAL and 4CL, to 25- to 60-fold higher activity for COMT, CCOMT, EOMT, and CVOMT. It is interesting that these ratios for COMT and CCOMT were not very different for the two lines (see "Discussion"). PAL activity was barely detectable in whole leaf extracts from the SW line, but was higher in the peltate glands of SW than in glands from EMX-1. EOMT and CVOMT activities were detectable not only in the EMX-1 leaves and peltate glands, but also in the SW peltate glands, although at much lower levels (approximately 130-fold) than in EMX-1 glands (Table I). This result explains the very low levels of methyleugenol found in this basil line.

We evaluated further the localization of the enzyme activities by assaying individual leaves that had been given the same abrasive treatment to (partially) remove the glands from the abaxial and adaxial leaf surfaces as had been performed to analyze essential oil content (see above and Fig. 4). The specific activities for PAL, 4CL, COMT, CCOMT, EOMT, and CVOMT in whole individual leaves and in individual leaves with the glands partially removed were determined. The ratios of specific activity (intact leaves compared with leaves abraded to remove glands) are shown in Figure 6B. For PAL in line EMX-1, for 4CL in line SW, and for COMT in both lines, these ratios are not significantly greater than 1, indicating that the majority of the activity for these enzymes is probably not found in the peltate glands, but elsewhere in the leaf. It is important to note that since the glands constitute a very small portion of the total mass of the leaf, it is possible to have much higher specific activity for a given enzyme in the glands than in the rest of the leaf and still have most of the activity found in the non-gland portion of the leaf. For 4CL in line EMX-1 and CCOMT in both basil lines, however, the ratios are between 1.5 and 2, and for EOMT and CVOMT activities in the EMX-1 line, the ratios are greater than 2, indicating that a large proportion of the activities of these enzymes is localized in the glands.

Peltate Glandular Trichomes Are Rich in mRNAs Encoding Phenylpropene-Related Biosynthetic Enzymes

Sequence analysis of 103 randomly chosen cDNAs from a library constructed from basil whole-leaf mRNAs revealed no sequences known to be involved in the phenylpropanoid pathway. Instead, most cDNAs encoded proteins involved in gene expression (17%), photosynthesis (16%), or unknown functions (19%; data not shown), with chlorophyll a/b-binding protein being the most highly expressed single cDNA (8%). We therefore prepared and analyzed a cDNA library from mRNAs obtained from peltate gland cells from line EMX-1. A total of 1,344 random cDNAs from this library were sequenced from their 5′ ends. Of these, 1,215 (or 90.4%) yielded high quality sequences. The mean and median size for the resulting expressed sequence tags (ESTs), after editing to remove vector sequences and poor quality 3′ sequences, were 552 bp (SD of 237 bp) and 525 bp, respectively, which correspond well with other reported EST databases (Lange et al., 2000).

Figure 6. Peltate glandular trichomes in basil lines EMX-1 and SW are highly enriched for enzymes in the phenylpropanoid pathway. A, Comparison of the ratios of enzymatic-specific activities present in crude extracts from peltate glands with specific activities present in crude extracts from whole young leaves. B, Comparison of enzymatic-specific activities present in crude extracts from whole young leaves with specific activities present in crude extracts from young leaves with leaves abraded to remove glands. White bar, EMX-1; diagonal-line filled bar, SW.
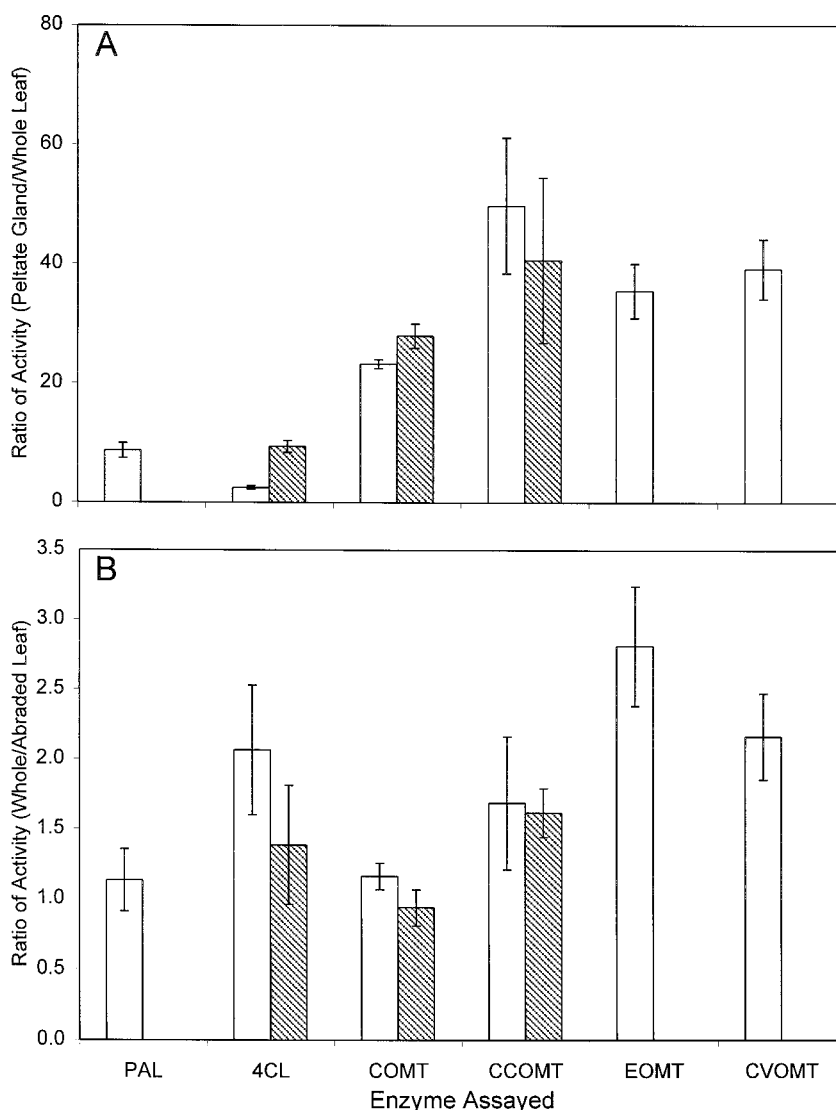
Some ESTs were shorter than 200 bp, and were mainly from 5′-truncated cDNAs, whereas others exceeded 1,000 bp in length. Fragment assembly identified a total of 656 contiguous sequences (contigs). Of these, 185 (or 28.2% of the contigs) contained two or more clones and were assembled from 745 (61.3%) of the total ESTs. The remaining 471 contigs contained only a single unique sequence (38.7% of total ESTs). Most of the contigs containing more than one sequence were of low abundance: 135 (or 20.6% of contigs) of the contigs contained two to four sequences (339 total sequences, 27.9% of total ESTs), 38 (or 5.8% of contigs) contained five to 10 sequences (255 total sequences, 21% of total ESTs), and 12 (or 1.8% of contigs) contained 11 or more sequences (151 total sequences, 12.4% of total ESTs). The largest number of sequences in a single contig was 17. This is significantly lower than the largest contigs obtained from the mint gland library (Lange et al., 2000), indicating that the basil peltate glands may be more complex than the mint glands, at least at the biochemical/molecular level. This observation is supported by the larger diversity of constituents found in the essential oil of basil.

ESTs were compared against GenBank and dbEST and were tentatively identified according to presumed biochemical function of the encoded proteins by comparison with the three highest matches in the databases. ESTs were then classified into 15 separate categories based on general physiological function (Fig. 7). A significant number of ESTs (35%) had no known function. This number is the sum of the ESTs that show homology to functionally undefined genes from other species (22%) and those ESTs showing no homology to anything in the databases (13%). This is comparable with the level of unknown genes in the poplar xylem and mint gland EST databases (Allona et al., 1998; Sterky et al., 1998; Lange et al., 2000). It is interesting that two of the most highly expressed single transcripts (contigs) in the basil gland data-
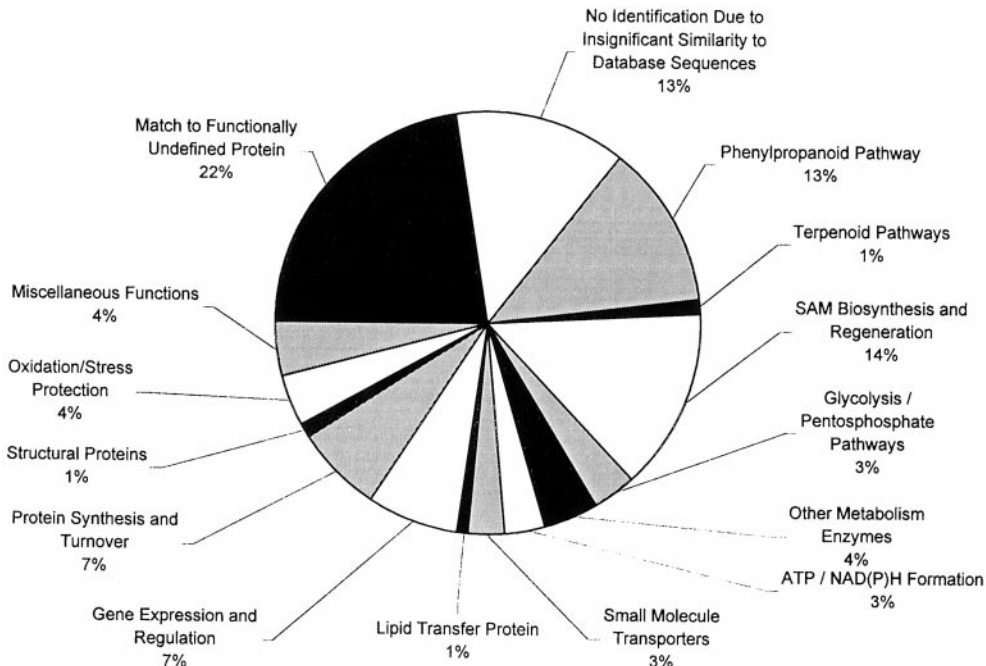
Figure 7. Abundance of physiological functional classes identified in the basil peltate gland EST database.

base, with 17 and 15 members in their respective contigs, encode proteins of unknown function.

The two largest categories of known enzymes identified in the basil EST gland database are directly involved in the formation of phenylpropenes. The first is the group of enzymes known to be involved in the formation and metabolism of *p*-coumaric and ferulic acids (designated as phenylpropanoid enzymes in Fig. 7). The enzymes in the second group are involved in the biosynthesis and regeneration *S*-adenosylmethinone (SAM), which is a substrate in the final reaction in the formation of the major essential oil constituent, methylchavicol, of this basil line and may also be involved in an earlier step in the pathway (see Fig. 1). Thus, a total of 62 and 35 ESTs were found to encode *S*-adenosyl-Met synthetase and *S*-adenosylhomo-Cys hydrolase, respectively, although these two types of ESTs were heterogeneous; each type appeared to represent several (>6) closely related isoforms/alleles, and were not the products of a single locus. Other genes in the phenylpropanoid pathway and SAM biosynthesis or utilization (e.g. CCOMT) were also very highly expressed (Table II).

To evaluate whether the abundance of a particular EST in the basil gland database corresponds to its level of expression in situ we analyzed the expression levels of two genes coding for enzymes in the phenylpropanoid pathway: CCOMT and COMT. CCOMT, with 28 transcripts from eight very similar isoforms (2.30% of total transcripts), was present in the basil gland EST database at very high levels. COMT, on the other hand, was present at much lower levels (0.08% of total transcripts). This many-fold difference in EST

abundance in the database correlates well with the level of transcripts found for these genes in northern blots (Fig. 8). Similar results were obtained with PAL and other phenylpropanoid-related genes (data not shown).

DISCUSSION

Our analysis of the location of the basil leaf phenylpropenes indicates that most, if not all, of the essential oil is found on the surface of the leaf (Fig. 4). In basil, the leaf surface, as well as the stem, sepals, and floral surfaces are covered with several types of structures that include hairy trichomes, peltate glands, and capitate glands. We have been able to separate and isolate the two types of glands, and to assay them for phe-

Table II. *The most abundant ESTs in the basil database with strong similarity to proteins with known function*

Putative EST Identification	Total No. of ESTs	Percent of Total ESTs
S-Adenosylmethionine synthetase	62	5.27
S-Adenosylhomocysteine hydrolase	35	2.97
Caffeoyl-CoA-*O*-methyltransferase	28	2.38
Glycine hydroxymethyltransferase	28	2.38
Cobalamine-independent methionine synthase	19	1.61
trans-Cinnamate 4-monooxygenase	18	1.53
Cinnamyl alcohol dehydrogenase	17	1.44
Caffeoyl-CoA *O*-methyltransferase-like	16	1.36
4-Coumarate:coenzyme A ligase	10	0.85
Glycine dehydrogenase (decarboxylating)	9	0.76
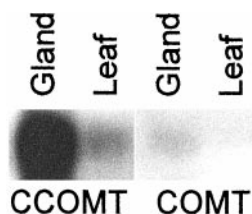
Figure 8. Northern-blot analysis of the relative abundance of mRNA transcripts for CCOMT and COMT in the peltate glandular trichomes (Gland) and young leaves (Leaf) of basil line EMX-1. Ethidium bromide staining (not shown) verified that equal amounts of total RNA (4 μg) were loaded per lane in the gel.

nylpropene content. Our results demonstrate that the capitate glands, which are more numerous than the peltate glands on the leaf surface though much smaller, do not store these compounds and do not possess the enzymatic activities necessary for methylchavicol and eugenol biosynthesis, although they are metabolically active. In contrast, we were able to show that the peltate glands do store these compounds. It is unfortunate that it is not possible to determine the exact proportion of the essential oil found in intact isolated glands compared with the total amount found in whole leaves. This is so because of the difficulty in correlating the amount of isolated glands with the amount of starting leaf material due to gland loss during the isolation protocol, because of the non-quantitative removal of the glands from the leaves (not all glands are removed from the leaves), and because of the loss of essential oil from gland sacs ruptured during the gland isolation procedure. However, the data from our studies on the effect of manual abrasive removal of the glands from the leaf surface (see Fig. 4), which correlated the level of oil content reduction with the relative reduction in number of glands on the leaf surface, indicate that most (if not all) of the essential oil is found on the surface of the leaf and that this oil is most likely restricted to the peltate glands. In addition, the composition of the oil found in intact peltate gland sacs and in isolated peltate glands is very similar to the composition of the oil extracted from intact leaves. These lines of evidence strongly support the conclusion that the intact peltate glands are the major site of phenylpropene accumulation in basil leaves.

The much higher levels (10- to 60-fold) of specific activity of the several phenylpropene pathway enzymes found in the isolated peltate glands compared with whole leaves (Table I; Fig. 6A) indicate that these glands are most likely the site of most, if not all, of the synthesis of the phenylpropenes in basil leaves. It is interesting that the specific activity of CCOMT in the peltate glands is 40- to 50-fold higher than in whole intact leaf tissue, whereas COMT specific activity is only 20- to 25-fold higher. Because the specific activity of CCOMT in whole-leaf extract is already 2-fold higher than that of COMT, this means

that in the peltate glands CCOMT-specific activity is at least 4-fold higher than that of COMT. This difference is consistent with the northern blotting data that show higher levels of CCOMT transcripts in peltate glands (Fig. 8), and it suggests that CCOMT may be more important in phenylpropene biosynthesis, although perhaps both are involved. The explanation for the similar levels of CCOMT and COMT activities in EMX-1 and SW lines is not only that EMX-1 plants make a small amount of methyleugenol, but also that both lines accumulate the less volatile coniferyl aldehyde and coniferyl alcohol in the peltate glands (data not shown), both of which contain a 3-methyoxy group.

The results showing a high level of phenylpropanoid/phenylpropene biosynthetic enzymes in peltate glands are concordant with the analysis of more than 1,200 cDNAs from the peltate glands, showing that transcripts encoding metabolic enzymes leading to the synthesis of the phenylpropenes are found there in high proportion. A detailed analysis of the types and frequencies of the cDNAs represented in this sampling suggests that the peltate glands are capable of synthesizing phenylpropenes and terpenes from Suc (see Fig. 9), and that these glands are highly specialized for these two pathways. Roughly two-thirds of the known enzymes required to convert Suc into phenylpropenes and terpenes have been identified among the 1,215 ESTs, and together they account for one-third (34%) of all transcripts and 84% of the transcripts encoding known enzymes. Additional enzymes participating in the phenylpropene (and terpene) pathways are likely to be represented in the "unidentified" class of ESTs, which presently accounts for 25% of the total.

Of special note is the high frequency of cDNAs encoding SAM-generating enzymes. Whereas SAM is needed for at least one, and possibly more, step(s) in the biosynthesis of phenylpropenes and other phenylpropanoids, this unusually high occurrence nonetheless raises the possibility that SAM is utilized in other pathways in the glands. However, which specific pathways these may be is not clear, since no cDNAs were found that encode enzymes that utilize SAM, such as for ethylene biosynthesis or for nucleic acid methylation.

In conclusion, the peltate glands appear to be the major, and possibly the only, site of phenylpropene storage and biosynthesis in basil leaves. Moreover, these glands appear to devote the majority of their metabolic activity to the synthesis of these phenylpropanoid volatile essential oil constituents, and they also transcribe the genes encoding the enzymes of this pathway at very high rates. Thus, these glands constitute a very simple biochemical and in vivo model system to study the phenylpropene pathway and its regulation, much as the peltate glands of mint constitute an excellent model system for terpene biosynthesis (Gershenzon et al., 1992; McCaskill et al., 1992; McCaskill and Croteau, 1995, 1999; Turner et
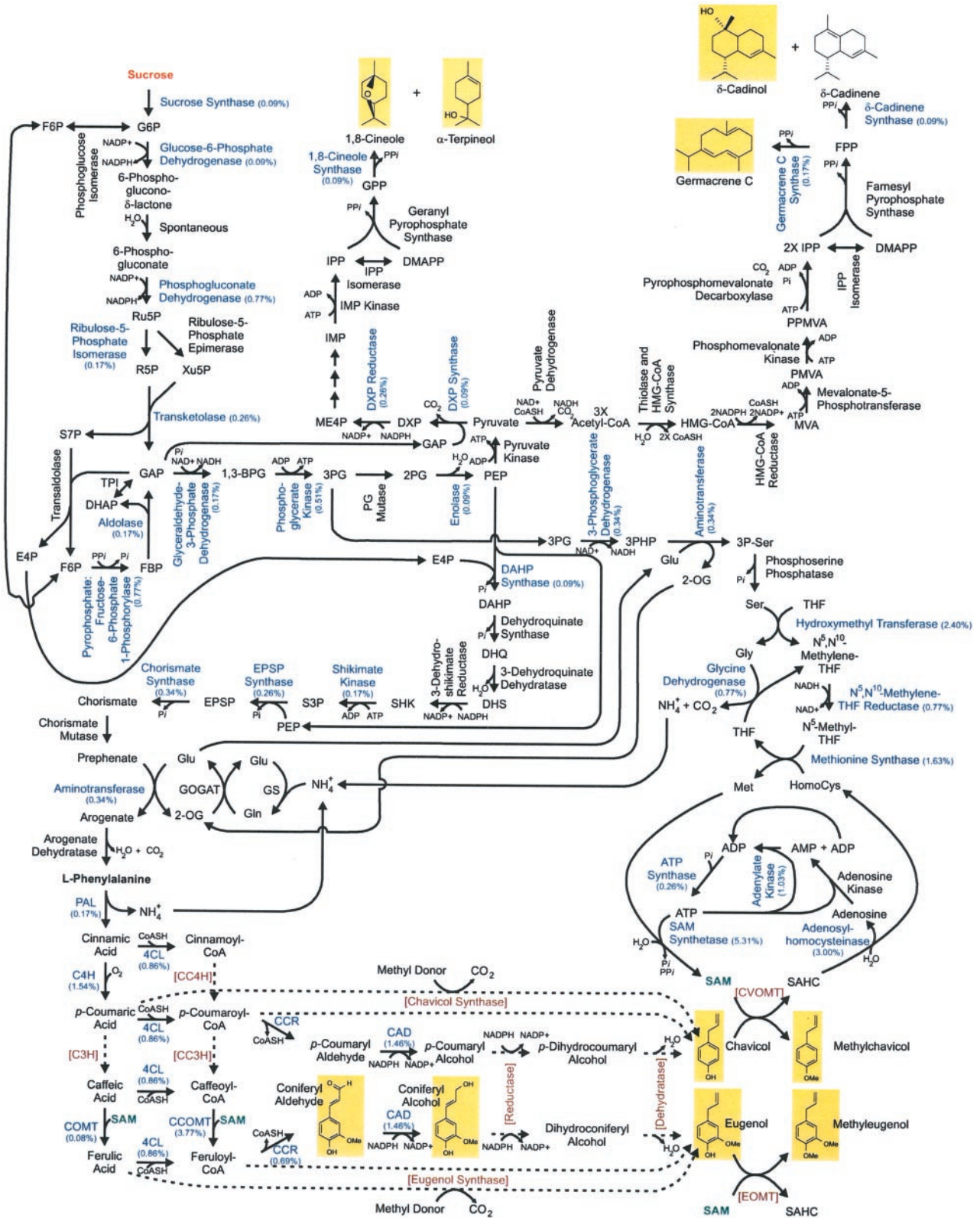
Figure 9. Network of metabolic pathways leading from Suc (orange, top left) to the volatile phenylpropanoids, phenylpropenes, and terpenoids formed in EMX-1 basil peltate glands (outlined with yellow backgrounds). Blue, Enzymes for which cDNAs have been identified in the basil peltate gland EST database, with the relative proportions in the database indicated in parentheses. Black, Known enzymes for which cDNAs have not yet been identified in the database. Red with brackets, Proposed enzymes in phenylpropene pathway for which genes are yet to be identified. Dashed lines, Hypothesized conversions. Green, SAM, an important substrate for phenylpropene biosynthesis.

al., 2000a, 2000b). In addition, since the peltate glands of the SW line produce high levels of the monoterpene linalool, as well as high levels of the phenylpropene eugenol, these glands would be an excellent model system to study the simultaneous regulation and modulation of flux into and through two important pathways in plant secondary metabolism.

MATERIALS AND METHODS

Plant Material

Seeds for two lines of basil (*Ocimum basilicum*), designated EMX-1 and SW, were from stocks developed at Newe Ya'ar Research Center, Israel. Seeds were sown directly into 1-L pots (four seeds per pot) or flats (40 seeds per flat) containing Sunshine Mix no. 1 potting soil. The soil was kept damp under controlled conditions at 25°C (constant temperature) in a growth chamber (CLD 3023, Conviron, Winnipeg, Manitoba, Canada) with 18-h light: 6-h dark cycle until seedlings emerged (about 10 d), after which time plants were grown under the same conditions or transferred to a greenhouse and grown under constant illumination and watered every other day with fertilizer (20:20:20) application once a week.

Reagents

All solvents and reagents were molecular biology grade or reagent grade or better and were obtained from Sigma St. Louis), Aldrich (Milwaukee, WI), or Fisher Scientific (Loughborough, Leicestershire, UK). Radiolabeled compounds were purchased from Sigma ([U-^{14}C]L-Phe) and ICN (*S*-[*methyl*-^{14}C]adenosyl-L-Met). [8-^{14}C]*p*-Coumaric acid was synthesized at 0.192 mmol scale from 4-hydroxybenzaldehyde and [2-^{14}C]malonic acid (Amersham, Buckinghamshire, UK) according to a previously reported method (Gagnaire and Robert, 1977), with a radiochemical yield of 71%.

Instrumentation

GC/MS was performed on a GC/MS system (QP-5000, Shimadzu, Columbia, MD) equipped with an Econo-Cap SE-54 capillary column (30 m × 0.32 mm i.d., 1.0-μm film thickness, Alltech, Deerfield, IL). Ultrapure helium was used as the carrier gas at a flow rate of 1.5 mL/min, with column pressure set at 10.4 kPa. The column was pre-equilibrated to 50°C, with the injector set at 250°C and the interface set at 280°C. Elution of compounds was achieved, after a 2 min hold at 50°C, by a linear temperature gradient from 50°C to 275°C in 22.5 min, with ionization performed in electron impact mode. Detection of mass ions and fragments was achieved with the detector set at 1.4 kV. Identification of eluted sample compounds was obtained by comparison of retention times and of fragmentation patterns with the NIST62 library. Single factor ANOVA) was performed using Microsoft Excel 2000.

HPLC was performed using a NovaPak C$_{18}$ column (30 cm × 4.6 mm i.d., Waters, Milford, MA) attached to a HPLC system (Shimadzu), containing an SCL-6A system controller, two LC-6A liquid chromatograph pumps, an ANS-3112 in-line degasser, a SIL-6A autoinjector, a CTO-6A column oven, a SPD-6AV UV-Vis spectrophotometric detector, and a C-R4A chromatopac analysis module. Complete baseline separation of all phenylpropene and phenylpropanoid compounds was done by modifying a previously reported method (Anterola et al., 1999). The flow rate was 1 mL min^{-1} and the column was incubated at constant temperature of 40°C, allowing for fast elution of the compounds of interest, but yielding excellent separation of eluted compounds. Solvent A was 3% (w/v) acetic acid in water; solvent B was 100% (w/v) acetonitrile. The column was pre-equilibrated with 3% B in A. After injection of up to a 25-μL sample, the column was washed with 2 mL of pre-equilibration solvent. Phenylpropanoids and phenylpropenes were eluted from the column with a linear gradient from 3% to 66% B over 50 mL. The column was then washed by increasing B to 95% (linear gradient in 2 mL) and holding at 95% B for 3 min. The column was then re-equilibrated by returning the column to 3% B (over 3 mL) followed by a 10-mL wash with this solvent. Total run time was 70 min. Fractions to be evaluated for radiochemical incorporation were obtained using a fraction collector (Gilson, Middleton, WI). One-half of each fraction was counted in a scintillation counter (Beckman Instruments, Fullerton, CA) in 2.5 mL of BioSafe II (Fisher) scintillation fluid.

Scanning Electron Microscopy (SEM)

Several different tissue samples from each basil line were prepared for SEM. These included very young leaves (less than 1 cm long), medium aged leaves (2–3 cm long), old leaves (greater than 4 cm long), flowers, shoot tips, and new inflorescences. Tissue was placed in 20-mL glass vials and was fixed by covering with 4% (w/v) glutaraldehyde, 25 mM NaHPO$_4$ (pH 7.0), and was incubated at 4°C overnight. Samples were then washed briefly with 25 mM NaHPO$_4$ (pH 7.0) and then transferred to new glass vials. The tissue was completely covered with a solution of 1% (w/v) osmium tetroxide in 25 mM NaHPO$_4$ (pH 7.0) and incubated at 4°C until the tissue turned completely black (approximately 4 d). The tissue was dehydrated through a series of 15-min incubations at room temperature (22°C–25°C) of 15%, 30%, 50%, 70%, 85%, and 95% (w/v) ethanol in water followed by 100% (w/v) ethanol. The 100% (w/v) ethanol was replaced by fresh ethanol and the samples were tightly capped and incubated overnight at room temperature. The ethanol was removed by critical point drying using liquid CO$_2$ in a Pelco CPD2 model 2400 Critical Point Drier (Dell Penna, Inc., Redding, CA). Samples were mounted onto aluminum disc mounts using colloidal silver paste (Dell Penna, Inc.) and gold coated at 50 mTorr and 40 mA in a Desk II gold sputtering machine (Denton Vacuum, Inc., Moorestown, NJ).

SEM images were obtained on a variable-pressure scanning electron microscope (S-3200 N, Hitachi, Tokyo) under very low pressure using the secondary electron scintillation detector and 20 kV accelerating voltage. Images were processed and scale bars were added using Quartz PCI Scientific Image Management System software, version 4.00.

Light Microscopy

Young leaves (0.5–1 cm in length) were prepared for sectioning and mounted on slides for light microscopic observation (Drews et al., 1991). To stain the tissue, slides were soaked in xylenes to remove the paraplast and were then fully hydrated through an ethanol:water series. After hydration tissues were stained with 0.1% (w/v) toluidine blue in water for 1 min and washed with water three times. Slides were next taken through the reverse ethanol:water series to fully dehydrate and were then finally soaked in xylenes before cover slips were attached. Light micrographs were obtained through a light microscope (Optihot-2, Nikon, Tokyo) using T-64 film (Kodak, Rochester, NY).

Samples of isolated glands for light microscopy were stained by adding 20% (v/v) of 2% (w/v) toluidine blue in water directly to isolated glands (in 10 μL of gland isolation buffer) spotted onto slides immediately after gland isolation, without prior or post-fixation or dehydration. Cover slips were placed and light micrographs were obtained immediately.

Gland Isolation

Peltate and capitate glandular trichomes were isolated from young leaves using a method modified from (Gershenzon et al., 1992). In brief, 15 g of new young leaves less than 2 cm in length were picked from growing stems using jewelers' forceps, placed in a 300 mL beaker (kept on ice), and soaked in ice-cold deionized water for 0.5 to 1 h to facilitate leaf swelling and gland removal. The water was decanted and the leaves were transferred to the 300-mL beveled flask supplied with a Bead Beater model 1107900 (Biospec Products, Inc., Bartlesville, OK) along with 40 to 50 g of glass beads (0.5 mm in diameter, Biospec Products, Inc.) and approximately 250 mL of ice-cold gland isolation buffer (50 mM Tris-HCl, 200 mM d-sorbitol, 20 mM Suc, 14 mM β-mercaptoethanol, 10 mM KCl, 5 mM MgCl$_2$, 0.5 mM K$_2$PO$_4$, 5 mM succinic acid, 1 mM EGTA, 0.6% [w/v] methylcellulose, and 1% [w/v] polyvinylpyrrolidone, 360,000 M$_r$). The Teflon beater blades were inserted into the beveled flask and the whole apparatus was tightly sealed and covered with ice in water to keep cold. The bead beater was plugged into a rheostat to supply constant low voltage to prevent the beating from becoming too violent. Glands were removed from the basil leaves with three pulses of 1 min at 30 V, with a 1-min rest between pulses. The glands were then separated from leaf material by passing the resulting mixture consecutively through a 350-μm mesh cloth (Small Parts, Inc., Miami Lakes, FL, to separate out leaves and glass beads) and a 105-μm mesh cloth (to remove leaf debris). Up to 300 mL of final of ice-cold gland storage buffer (gland wash buffer without addition of methylcellulose or polyvinylpyrrolidone) was added during the gland isolation procedure to facilitate flow and to wash the glands through the mesh cloths. The peltate glands (average of 80 μm in diameter) were collected on a 40-μm mesh cloth, which allowed the capitate glands to pass through, which were then collected on a 20-μm mesh cloth (average of 30 μm in diameter). Collected glands were washed at least eight times on the mesh cloth with ice-cold gland storage buffer, transferred to a 1.5-mL microcentrifuge tube, and placed on ice to settle. Yield was about 300 μL (packed gland volume) of peltate glands and about 50 μL of capitate glands per 15 g of leaf sample.

Volatile Oil Characterization

Individual peltate glands were analyzed for essential oil constituents by piercing the gland oil sac ("subcuticular space") with a stretched glass pipette. The small droplet of oil thus obtained was removed by placing the pipette in 60 μL of ethyl acetate in a small glass vial insert. Three microliters of the resulting solutions were analyzed by GC/MS for determination of the major oil constituents.

Essential oil composition of whole leaves was analyzed by soaking whole or ground leaves in 1 mL of MTBE for 1 to 12 h in 5-mL glass vials sealed with rubber septa caps and wrapped with Parafilm M (American National Can, Norwalk, CT), or by soaking in 0.5 mL of MTBE overnight in microfuge tubes (which gave comparable results). Toluene was added as an internal standard and the resulting extract, if used for qualitative analysis, was concentrated to approximately 20 μL under dry nitrogen and dissolved in 80 μL of ethyl acetate. Three microliters of the resulting solutions were analyzed by GC/MS for determination of the essential oil constituents. Extracts made with hexanes, ethyl acetate, acetone, or methanol all gave essential oil profiles comparable with those obtained from extraction with MTBE, but contained large amounts of waxes or chlorophyll. Thus, MTBE was found to be a better solvent for essential oil extraction and analysis. For quantitative determination of the major essential oil constituents, small basil leaves (1–2 cm in length) were individually transferred to microcentrifuge tubes, weighed, and extracted with MTBE, with 0.003% (w/v) toluene added as an internal standard. One-half of the leaves were ground in the solvent mixture using a stainless steel microhomogenizer attached to a hand drill. One-third of the leaves were also abraded (after weighing and prior to transfer to microfuge tubes) with a cotton swab to remove glands. These leaf samples were then rinsed three times with 100% (w/v) ethanol and extracted as above. None of the extracts obtained in microfuge tubes for quantitative determination were concentrated by evaporation prior to GC/MS analysis.

The essential oil composition of the isolated glands (peltate and capitate) was determined by extracting 50 μL of packed gland volume two times with 100 μL of MTBE or ethyl acetate, followed by concentration, and GC/MS analysis as above.

Enzyme Assays

Soluble protein extracts were made from young leaves. Whole individual leaves (1–2 cm in length) were weighed and placed in 1.5-mL microcentrifuge tubes. Ice-cold protein extraction buffer (10:1, w/v), consisting of 50 mM BisTris [2-[bis(hydroxyethyl)amino]-2-(hydroxymethyl)-1-propane-1,3-diol]HCl, pH 8.0, 14 mM β-mercaptoethanol, and 10% (w/v) glycerol, was added and the leaves were ground using a stainless steel microhomogenizer attached to a hand drill. After incubation on ice for 30 min, the protein extract was obtained by centrifuging the ground mixture at

14,000g for 20 min at 4°C and transferring the clarified supernatant to a new tube. For stripped individual leaves, single leaves were abraded with a cotton swab to remove glands after weighing and prior to extraction as above. Soluble protein extracts were made from peltate or capitate glands by resuspending isolated glands in ice-cold 10:1 (v/v) protein extraction buffer and sonicating on ice for a maximum of 30 s until gland secretory cells had lysed (which was verified by light microscopic inspection of a small amount of the lysed mixture). Care was taken to prevent the protein solution from becoming warm during the sonication. The gland protein extracts were obtained by centrifugation as for the leaf extracts. For stripped batched leaves, one-half of the leaves remaining after gland isolation procedure (or 7.5 g) were rinsed well with deionized water and extracted with 3× protein extraction buffer as for whole batched leaves. Protein extracts were used immediately or stored at −20°C until needed.

PAL activity was determined using two methods that gave comparable results. The first method, based on a previously reported method (Zucker, 1965; Lamb et al., 1979), measures the change in A_{290} as L-Phe is converted to cinnamic acid, using the extinction coefficient for trans-cinnamic acid of 10,000 M^{-1} cm^{-1}. The extinction coefficient for Phe is approximately 0 at 290 nm. In a 1.5-mL methacrylate spectrophotometer cuvette, in a final assay volume of 0.8 mL were added: 0.1 M sodium borate, pH 8.8, and L-Phe to a final concentration of 1 mM. To initiate the assays, 4 μL of protein extract (containing approximately 100 μg of protein) were added and the cuvettes were sealed and mixed by gentle inversion. The reaction was followed at room temperature for several hours. Controls included assays of boiled protein extracts with all reaction components, of all reaction components without protein added and of all components except for L-Phe substrate, all of which showed no activity.

Because the spectrophotometric assays were not very sensitive and required long monitoring times, a second assay was developed that measures the conversion of [U-^{14}C]L-Phe into [U-^{14}C]cinnamic acid. In a 1.5-mL microfuge tube, in a final assay volume of 50 μL were added: 0.1 M sodium borate, pH 8.8, [U-^{14}C]L-Phe (1 μM, 460 mCi/mmol, Sigma), and 20 uL of protein extract diluted to 0.25 μg/μL, for a total of 5 μg of protein per assay. Assays were initiated by addition of protein to the other reaction components and allowed to incubate at room temperature for 1 h. Controls included assays of boiled protein extracts containing all reaction components and assays of all reaction components without protein added. Product was extracted by adding 5 μL of 6 N HCl and 100 μL of ethylacetate, vortexing, and centrifuging at 14,000g for 3 min. Radiochemical incorporation rates were determined by scintillation counting of 40 μL of the ethylacetate phase. Product identification was verified by HPLC where the radiolabeled product co-eluted with known standard.

EOMT activity was determined by measuring the formation of radiolabeled methyleugenol from eugenol and S-[methyl-^{14}C]adenosyl-L-Met by protein extracts from isolated gland and whole leaves (0.1 and 10 μg of total pro-

tein, respectively, for gland and leaf protein extracts, diluted if necessary in extraction buffer; Wang and Pichersky, 1998). CVOMT and COMT activities were determined as for EOMT, with substitution of chavicol and caffeic acid, respectively, for eugenol as substrate. CCOMT activity was determined as for EOMT, except that caffeoyl-CoA was substituted for eugenol as substrate and, prior to acidification (with 16 μL of 6 N HCl) and extraction with ethylacetate, the hydroxycinnamoyl CoA esters were hydrolyzed by base treatment (5 μL of 10 N NaOH added, heating at 70°C for 10 min). For all O-methyl transferase activities, controls were as for PAL assays, all of which showed no activity (as measured by radiochemical incorporation into ethylacetate extractable products). An additional control for CCOMT activity included assays that were not base hydrolyzed, and these showed no activity. Authenticities of radiolabeled assay products (for PAL, COMT, CCOMT, EOMT, and CVOMT activities) from assays involving radiochemicals were determined by co-elution with known standards on HPLC.

4CL activity was determined measuring the formation of [8-^{14}C]p-coumaroyl-CoA from [8-^{14}C]p-coumaric acid (1.56 mM, 45,000 dpm/assay) and CoA (0.4 mM) in the presence of 2.5 mM ATP, 5 mM MgCl$_2$, and 5 μg of protein extract in a 50-μL final volume of 50 mM Tris-HCl, pH 7.5. After a 1-h incubation at room temperature, assays were stopped by adding 3 μL of 6 N HCl and extracting with 100 μL of ethylacetate, which was removed after centrifugation for 3 min at 14,000g. An additional 100 μL of diethyl ether was used for extraction, and this was completely removed by freezing the centrifuged samples at −80°C and removing the overlaying solvent, whereas the aqueous phase remained frozen. The aqueous and the combined organic fractions were then separately analyzed by scintillation counting for radiolabel incorporation. Controls included assays with boiled protein extracts and assays with no CoA added, both of which gave low background counts.

Malate dehydrogenase activity was determined spectrophotometrically. In brief, in a 1.5-mL cuvette in a final volume of 0.8 mL were added 50 mM Tris-HCl, pH 7.5, 500 μM NAD$^+$, 1 mM malic acid, and 2.5 μg of protein extract. The reaction was monitored in a spectrophotometer at 340 nm. Controls included assays with no protein and assays without addition of malic acid.

cDNA Library Construction

A cDNA library from whole young leaf tissue from line EMX-1 was previously prepared (Wang et al., 1999). For the construction of a cDNA library from peltate glandular trichomes, we chose line EMX-1 because this line contains eugenol- and chavicol-derived phenylpropenes, as well as several terpenoids in its essential oil described herein. The glands were isolated as described above, except that aurintricarboxylic acid (1 mM) was added to all buffers and solutions used and leaves were soaked in water (containing 1 mM aurintricarboxylic acid and 1 mM β-mercaptoethanol) after harvesting for 15 min prior to transfer to the bead beater. After the glands were washed from the 40-μm mesh cloth, transferred to a 1.5-mL microfuge tube, and allowed

to settle, the overlaying gland isolation buffer was removed. The yield was 250 mg of glands per 15 g of young leaves. One hundred milligrams of glands were immediately resuspended in 450 μL of buffer RLT (Qiagen, Valencia, CA) and lysed by a 30-s sonication pulse. Total RNA was purified using the RNeasy Plant Mini kit (Qiagen), with a yield of 51 μg of RNA per 100 mg of isolated glands. A directional cDNA library was constructed using the Uni-ZAP XR cDNA synthesis kit (Stratagene, La Jolla, CA) with 1 μg of Poly(A)$^+$ mRNA [isolated by the PolyATtract mRNA Isolation System, Promega, Madison, WI, with a yield of 1 μg of Poly(A)$^+$ mRNA per 332 μg of total RNA]. The original library had a titer of 8.9×10^6 plaque forming units (pfu). An aliquot (1×10^6 pfu) of this primary library was amplified, and the amplified library had a titer of 1×10^{13} pfu. PCR amplification of inserts of 40 random plaques (using T7 and T3 primers) indicated that the average insert size was approximately 1.0 to 1.5 kbp. Mass excision of pBluescript phagemids from the amplified library resulted in a stock with a total of approximately 1.8×10^8 colony forming units. This stock was used for plating and random colony picking for cDNA sequencing.

cDNA Sequencing

A total of 1,344 basil cDNAs were randomly and automatically isolated, and sequenced from their 5′ end (using the T3 primer). After vector and poor quality sequences were removed using the Lucy program (The Institute for Genomic Research), the resulting basil ESTs were compared with GenBank and dbEST using the BLASTX and TBLASTX search algorithms. The Institute for Genomic Research Assembler (14) was used for contig assembly and the ESTs were then assigned specific functions (gene identification) based on highest similarity, and categorized according to general functional category (e.g. phenylpropanoid metabolism, protein synthesis, etc.).

Northern Blotting

Total RNA (4 μg) from isolated peltate glandular trichomes and from young leaves was resolved on 1% (w/v) agarose-formaldehyde gels and blotted (Gang et al., 1999) to Hybond-N+ nylon membranes. Probes were synthesized using the ^{T7}QuickPrime kit (Amersham Pharmacia, Uppsala) from PCR-amplified fragments of basil CCOMT (approximately 400 bp), COMT (approximately 1,200 bp), and PAL (approximately 800 bp) cDNAs, which were identified in the EST database. Hybridization and washes at 65°C were performed under standard conditions (Sambrook et al., 1989).

ACKNOWLEDGMENT

LITERATURE CITED

Adams S, Weidenborner M (1996) Mycelial deformations of *Cladosporium herbarum* due to the application of eugenol or carvacrol. J Essential Oil Res **8:** 535–540

Allona I, Quinn M, Shoop E, Swope K, St. Cyr S, Carlis J, Riedl J, Retzel E, Campbell MM, Sederoff R, Whetten RW (1998) Analysis of xylem formation in pine by cDNA sequencing. Proc Natl Acad Sci USA **95:** 9693–9698

Anterola AM, van Rensburg H, van Heerden PS, Davin LB, Lewis NG (1999) Multi-site modulation of flux during monolignol formation in loblolly pine (*Pinus taeda*). Biochem Biophys Res Commun **261:** 652–657

Bala S, Sukul N (1987) Systemic nematocidal effect of eugenol. Nematropica **17:** 219–222

Bara M, Vanetti M (1995) Antimicrobial effect of spices on the growth of *Yersinia enterocolitica*. J Herb Spice Med Plant **3:** 51–58

Blank G, Al-Khayat M, Ismond M (1987) Germination and heat resistance of *Bacillus subtilis* spores produced on clove and eugenol based media. Food Microbiol **4:** 35–42

Bohlmann J, Meyer-Gauen G, Croteau R (1998) Plant terpenoid synthases: molecular biology and phylogenetic analysis. Proc Natl Acad Sci USA **95:** 4126

Boudet A-M, Goffner D, Marque C, Grima Pettanati J, eds (1998) Genes Involved in the Final Steps of Monolignol Biosynthesis and Their Manipulation for Tailoring New Lignins, Vol 697. American Chemical Society, Washington, DC, pp 65–75

Chappell J (1995) The biochemistry and molecular biology of isoprenoid metabolism. Plant Physiol **107:** 1–6

Charles D, Simon J, Wood K (1990) Essential oil constituents of *Ocimum micranthum* Willd. J Agric Food Chem **38:** 120–122

Chatterjee A, Sukul N, Laskar S, Ghoshmajumdar S (1982) Nematicidal principles from two species of Lamiaceae *Ocimum sanctum* and *Ocimum basilicum*. J Nematol **14:** 118–122

Drews GN, Bowman JL, Meyerowitz EM (1991) Negative regulation of the *Arabidopsis* homeotic gene AGAMOUS by the APETALA2 product. Cell **65:** 991–1002

Gagnaire D, Robert D (1977) Polymer model of lignin (DHP) C-13 selectively labeled at benzylic positions: synthesis and NMR study. Makromol Chem **178:** 1477–1495

Gang DR, Kasahara H, Xia Z-Q, Vander Mijnsbrugge K, Bauw G, Boerjan W, Van Montagu M, Davin LB, Lewis NG (1999) Evolution of plant defense mechanisms: relationships of phenylcoumaran benzylic ether reductases to pinoresinol-lariciresinol and isoflavone reductases. J Biol Chem **274:** 7516–7527

Gershenzon J, McCaskill D, Rajaonarivony JIM, Mihaliak C, Karp F, Croteau R (1992) Isolation of secretory cells from plant glandular trichomes and their use in biosynthetic studies of monoterpenes and other gland products. Anal Biochem **200:** 130–138

Gildemeister E, Hoffmann FR (1913) Ätherischen Öle. Pharmaceutical Review Publication Co., Milwaukee, WI

Grayer R, Kite G, Goldstone F, Bryan S, Paton S, Putievsky E (1996) Infraspecific taxonomy and essential oil

chemotypes in sweet basil, *Ocimum basilicum*. Phytochemistry **43:** 1033–1039

Guenther E (1949) The Essential Oils. D. Van Nostrand Company, Princeton, NJ

Karapinar M, Aktug S (1987) Inhibition of foodborne pathogens by thymol, eugenol, menthol and anethole. Int J Food Microbiol **4:** 161–166

Klischies M, Stockigt J, Zenk MH (1975) Biosynthesis of the allylphenols eugenol and methyleugenol in *Ocimum basilicum* L. Chem Commun **21:** 879–880

Lamb CJ, Merritt TK, Butt VS (1979) Synthesis and removal of phenylalanine ammonia-lyase activity in illuminated discs of potato tuber parenchyme. Biochim Biophys Acta **582:** 196–212

Lange BM, Wildung MR, Stauber EJ, Sanchez C, Pouchnik D, Croteau R (2000) Probing essential oil biosynthesis and secretion by functional evaluation of expressed sequence tags from mint glandular trichomes. Proc Natl Acad Sci USA **97:** 2934–2939

Lewinsohn E, Ziv-Raz I, Dudai N, Tadmor Y, Lastochkin E, Larkov O, Chaimovitsh D, Ravid U, Putievsky E, Pichersky E, Shoham Y (2001) Biosynthesis of estragole and methyl-eugenol in sweet basil (*Ocimum basilicum* L.): developmental and chemotypic association of allylphenol *O*-methyltransferase activities. Plant Sci **160:** 27–35

Manitto P, Granatica P, Monti D (1975) Biosynthesis of phenylpropanoid compounds: II. Incorporation of specifically labeled cinnamic acids into eugenol(*Ocimum basilicum*). J Chem Soc Perkin Trans I **16:** 1549–1551

Manitto P, Monti D, Gramatica P (1974) Biosynthesis of phenylpropanoid compounds: I. biosynthesis of eugenol in *Ocimum basilicum* L. J Chem Soc Perkin Trans I **14:** 1727–1731

Matsuoka H, Dousaki S, Kurata N, Homma T, Nemoto Y (1993) Effect of flavor compounds emitted by white birch on the seed germination of the same plant. J Plant Nutri **16:** 471–478

McCaskill D, Croteau R (1995) Monoterpene and sesquiterpene biosynthesis in gladular trichomes of peppermint (*Mentha × piperita*) rely exclusively on plastid-derived isopentenyl diphosphate. Planta **197:** 49–56

McCaskill D, Croteau R (1999) Isopentenyl diphosphate is the terminal product of the deoxyxylulose-5-phosphate pathway for terpenoid biosynthesis in plants. Tet Lett **40:** 653–656

McCaskill D, Gershenszon J, Croteau R (1992) Morphology and monoterpene biosynthetic capabilities of secretory cell clusters isolated from glandular trichomes of peppermint (*Mentha × piperita*). Planta **187:** 445–454

Miyao S (1975) Inhibitory effects of ethanol extract of mace and eugenol on the growth of microorganisms isolated from Vienna sausages. Nihon Shokuhin Eisei Gakkai **16:** 412- 416

Moleyar V, Narasimham P (1992) Antibacterial activity of essential oil components. Int J Food Microbiol **16:** 337–342

Navasero R, Ramaswamy S (1991) Morphology of leaf surface trichomes and its influence on egglaying by *Heliothis virescens*. Crop Sci **31:** 342–353

Obeng-Ofori D, Reichmuth C (1997) Bioactivity of eugenol, a major component of essential oil of *Ocimum suave* (Wild.) against four species of stored-product *Coleoptera*. Int J Pest Manag **43:** 89–94

Pareek S, Maheshwari M, Gupta R (1980) Domestication studies on *Ocimum sanctum* sweet basil for high oil and eugenol content. Indian Perfumer **24:** 93–100

Ryu D, Holt D (1993) Growth inhibition of *Penicillium expansum* by several commonly used food ingredients. J Food Protect **56:** 862–867

Sambrook J, Fritsch EF, Maniatis T (1989) Molecular Cloning: A Laboratory Manual, Ed 2. Cold Spring Harbor Laboratory Press, Cold Spring Harbor, NY

Sangwan N, Verman B, Verma K, Dhindsa K (1990) Nematicidal activity of some essential plant oils. Pest Sci **28:** 331–335

Senanayake UM, Wills RBH, Lee TH (1977) Biosynthesis of eugenol and cinnamic aldehyde in *Cinnamomum zeylanicum*. Phytochemistry **16:** 2032–2033

Shukla R, Prasad V (1985) Population fluctuations of the oriental fruit fly, *Dacus dorsalis* Hendel in relation to hosts and abiotic factors. Tropic Pest Manag **31:** 273–275

Sisk C, Shorey H, Gerber R, Gaston L (1996) Semiochemicals that disrupt foraging by the Argentine ant (Hymenoptera: Formicidae): laboratory bioassays. J Econ Entomol **89:** 381- 385

Sterky F, Regan S, Karlsson J, Hertzberg M, Rohde A, Holmberg A, Amini B, Bhalerao R, Larsson M, Villarroel R, Van Montagu M, Sandberg G, Olsson O, Teeri TT, Boerjan W, Gustafsson P, Uhlén M, Sundberg B, Lundeberg J (1998) Gene discovery in the wood-forming tissues of poplar: analysis of 5,692 expressed sequence tags. Proc Natl Acad Sci USA **95:** 13330–13335

Turner GW, Gershenzon J, Croteau RB (2000a) Distribution of peltate glandular trichomes on developing leaves of peppermint. Plant Physiol **124:** 655–663

Turner GW, Gershenzon J, Croteau RB (2000b) Development of peltate glandular trichomes of peppermint. Plant Physiol **124:** 665–679

Walters D, Harman J, Craig R, Mumma R (1991) Effect of temperature on glandular trichome exudate composition and pest resistance in geraniums. Entomol Exp Appl **60:** 61–69

Wang J, Dudareva N, Bhakta S, Raguso R, Pichersky E (1997) Floral scent production in *Clarkia breweri* (Onagraceae): II. Localization and developmental modulation of the enzyme *S*-adenosyl-ʟ-methionine:(iso) eugenol *O*-methyltransferase and phenylpropanoid emission. Plant Physiol **114:** 213–221

Wang J, Dudareva N, Kish CM, Simon JE, Lewinsohn E, Pichersky E (1999) Nucleotide sequences of two cDNAs encoding caffeic acid *O*-methyltransferases from sweet basil (*Ocimum basilicum*). Plant Physiol **120:** 1205

Wang J, Pichersky E (1998) Characterization of *S*-adenosyl-ʟ-methionine:(iso) eugenol *O*-methyltransferase involved in scent production in *Clarkia breweri*. Arch Biochem Biophys **349:** 153–160

Wang J, Pichersky E (1999) Only a few amino acid changes can interconvert two *O*-methyltransferases with different substrate specificities. Arch Biochem Biophys **368:** 172

Werker E, Putievsky E, Ravid U, Dudai N, Katzir I (1993) Glandular hairs and essential oil in developing leaves of *Ocimum basilicum* L. (Lamiaceae). Ann Bot **71:** 43–50

Wise MI, Savage TJ, Katahira E, Croteau R (1998) Mono-terpene synthases from common sage (*Salvia officinalis*): cDNA isolation, characterization, and functional expression of (+)-sabinene synthase, 1:8-cineole synthase, and (+)-bornyl diphosphate synthase. J Biol Chem **273:** 14891–14899

Zucker M (1965) Induction of phenylalanine deaminase by light and its relation to chlorogenic acid synthesis in potato tuber tissue. Plant Physiol **40:** 779–784.